 DOI:10.30420/566414030

The effect of the bonded interface damage on mechanical and electro-thermal characteristics of the IGBT Modules

Shengjun Zhao[1,2], Tong An [1,2], Fei Qin[1, 2]

[1] Institute of Electronics Packaging Technology and Reliability, School of Mathematics, Statistics and Mechanics, Beijing University of Technology, Beijing 100124, China

[2] Beijing Key Laboratory of Advanced Manufacturing Technology, Beijing University of Technology, Beijing 100124, China

Corresponding author: Tong An, antong@bjut.edu.cn

Speaker: Shengjun Zhao, sjzhao@emails.bjut.edu.cn

Abstract

For insulated gate bipolar transistor (IGBT) modules using wire bonding as the interconnection method, the primary failure mechanism is the cracking of the bonded interface. Studying the effect of the bonded interface damage on mechanical and electro-thermal characteristics is crucial for assessing the reliability of IGBT modules. This paper established these finite element models of IGBT modules with different bonded areas and conducted a two-step indirect coupling electro-thermal-mechanical analysis under power cycling. The analysis results show that the current density and the displacement of boding wires significantly increase with the increase of bonded interface damage.

1 Introduction

Insulated Gate Bipolar Transistor (IGBT) modules are widely used in various fields due to their fast-switching speed, low driving power consumption, and simple driving circuit [1], making them a critical component in power electronic systems. High-purity aluminum bonding wires, with diameters ranging from 125 μm to 500 μm, are commonly utilized for connecting IGBT chips to external circuits [2]. The wires are connected using an ultrasonic bonding process [3]. In practical applications, the bonded interface is subjected to cyclic thermal stresses due to the difference between the coefficients of thermal expansion (CTE) of the bonding wires and the Si chip. As service time increases, cracks can occur at the bonded interface and gradually expand. This can significantly affect the conductive and heat transfer properties of the IGBT module, ultimately leading to its failure [4]. Studies have shown that bonded interface damage is a primary cause of failure in IGBT modules [5]. Therefore, it is crucial to study the impact of bonded interface damage on the mechanical and electro-thermal characteristics to assess the reliability of IGBT modules.

The bonded interfaces have been studied primarily through experimental measurements or numerical simulations. Ayda [6] investigated the microstructure evolution of aluminum wires in IGBT modules during power cycling using electron backscatter diffraction (EBSD). The results reveal that fracture initiation occurs at the extremities of the bonded interface, and the cracks then gradually propagate as cycling proceeds towards the center of the bonded region and propagate strictly at the contact. In numerical simulation, many scholars have studied the thermal stress at the bonded interface for undamaged modules and the influence of bonding wire lift-off on electro-thermal characteristics [7]. However, these analyses do not match the actual damage state of the bonding wire during the power cycling, which can lead to significant errors in evaluating the electro-thermal characteristic parameters.

Given the discussion above, this paper studied the impact of bonded interface damage on the mechanical and electro-thermal properties of the IGBT module by numerical simulation. First, five finite element models of the IGBT module with different areas of bonded interface damage were established. It should be noted that these models were generated based on the birth and death element technique. Then, we accomplished a two-step indirect coupling electro-thermal-mechanical analysis for these models under power cycling. Finally, we analyzed the influence of bonded interface damage on the electro-thermal-mechanical parameters, which included turn-on voltage (V_{ce}), maximum temperature (T_{max}), current density, and displacement of the bonding wires. These studies provide theoretical guidance for a comprehensive understanding of the packaging failure of the IGBT module.

ISBN 978-3-8007-6414-3

 DOI:10.30420/566414030

2 Modelling Process

2.1 Geometry model of IGBT

In this paper, an IGBT module rated at 1200V/450A was utilized, comprising eight components including a plastic case, encapsulant, FWD and IGBT power semiconductor chips, bonding wire, baseplate, bonding material, and DBC substrate, as illustrated in Figure 1(a). This module is divided into an upper-half bridge and a lower-half bridge. Typically, only one-half bridge is operating during the power cycle. Therefore, we have established the geometric model in Figure 2 in this paper. Figure 2(b) is the schematic cross-section of the FE model, which shows baseplate, lower solder layer, lower copper layer, ceramic, upper copper layer, upper solder layer, IGBT silicon chip, FWD silicon chip, aluminum metallization layer, and aluminum bonding wires from bottom to top.

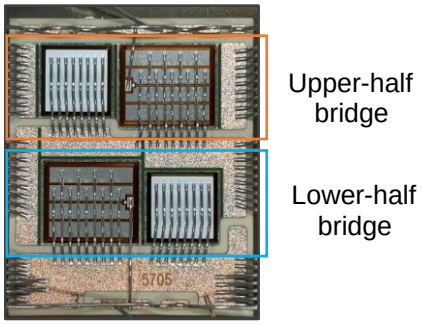

Fig. 1. The IGBT module

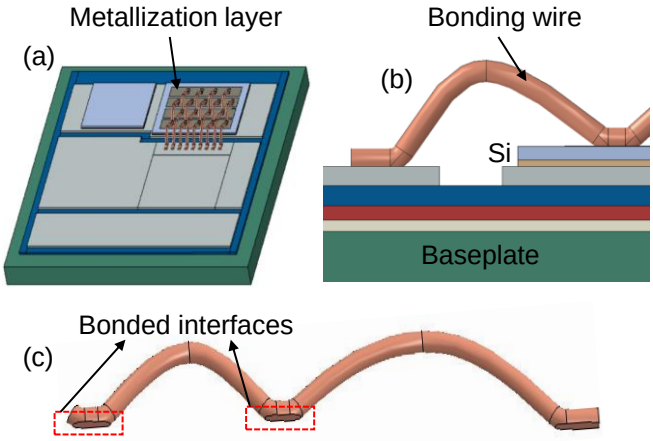

Fig. 2. The FE model of IGBT. (a) The geometry model; (b) The schematic cross-section; (c) Bonding wire

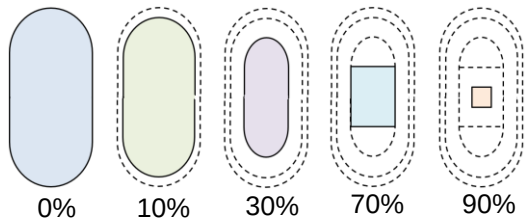

Fig. 3. Five damage state of Bonded interfaces

In the IGBT module, there are a total of 9 bonding wires. Each bonding wire has the same damage state, and the damage propagates from the outermost to the center of the bonded interface. The different bonded interface areas represent different damage states. Five damage states were established, as shown in Figure 3. The damage area ratio to the total area of the bonded interface is 0%, 10%, 30%, 70%, and 90%, respectively. The relevant geometric dimensions are summarized in Table 1. The size of the baseplate is shown in Fig. 2(a). The upper copper layer is divided into three parts, and the dimensions are 30×11.3×0.3 mm^3, 30×15.3×0.3 mm^3, and 30×7×0.3 mm^3, respectively. The cross-section of the bonding wire is circular, with a diameter of 0.4mm.

Table. 1. The dimensions of the IGBT module

Component	Dimension (mm×mm×mm)
Baseplate	36×43×3
Lower solder layer	30×37×0.2
lower copper layer	30×37×0.27
ceramic	32×39×0.37
upper solder layer	12.4×10.7×0.12
IGBT silicon chip	12.4×10.7×0.252
FWD silicon chip	9.2×9.3×0.252
Al metallization layer	10.4×2×0.0066 (number 4)

2.2 Mesh model and material property

The FE model is meshed by the swept method, which contains 105794 elements. The element type is DC3D8E for the electro-thermal simulation and C3D8R for the structure simulation. All materials are assumed to be isotropic. The material properties of each part in the FE model are shown in Table 2 [7]. The materials of the metallization layer and bond-wire are Al. In addition, the solder is SAC305, the IGBT and FWD chip is Si, the ceramic is Al_2O_3, and the baseplate is Cu.

2.3 Load and boundary condition

A two-step indirect coupling electro-thermal-mechanical analysis was conducted for the five models mentioned above. Namely, the electro-thermal simulation was performed to obtain the temperature field of the IGBT module. After that, the thermal-mechanical simulation was carried out to get the stress/strain field according to previous temperature results.

In the electro-thermal simulation, eight cycles of a cyclic current load, shown in Figure 4, were applied to the upper side copper layer, and the electric potential at the lower side copper layer was zero. The cyclic current load has an amplitude of 400 A, a cycle of 8 seconds, and a duty ratio of 0.5. The ceramic is regarded as an electric insulation body. For boundary conditions, an

equivalent convection coefficient of 3900 W/m^2·K was applied to the bottom of the baseplate. Moreover, the initial temperature was set at 45°C. After several cycles, the module's junction temperature will be stable.

In the thermal-mechanical simulation, the load is the temperature results obtained from the electro-thermal analysis. The stress-free reference temperature was set as 25°C. Assuming that the module's initial residual stress/strain is 0. For the boundary condition, the nodes at the bottom of the baseplate were fixed, i.e., the displacement of the bottom of the baseplate remained at 0 during the analysis process. It should be noted that the loads and boundary conditions are the same for different models in the electro-thermal and thermal-mechanical analysis.

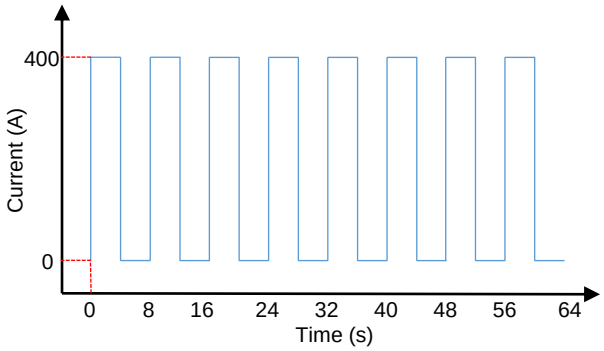

Fig. 4. Cyclic current load with an amplitude of 400A and turn on/off 4s/4s

Table. 2. Material properties

Material	Electrical Resistivity (mΩ·mm)	Thermal Conductivity (W/m·°C)	Specific Heat (J/kg·°C)	Density (kg/m^3)	coefficients of thermal expansion (ppm/°C)	Young Modulus (GPa)	Poisson's Ratio
Al	2.65×10^{-2}	237	900	2700	24	70.6	0.34
Si	2.1×10^{-4}	168	700	2330	2.5	130	0.22
Cu	1.7×10^{-2}	400	380	8920	17.3	128	0.36
Al_2O_3	1×10^{18}	20	753	3960	7.2	345	0.25
SAC305	1.04×10^{-1}	33	234	7400	30.2	15	0.4

3 Results and discussion

3.1 Electro-Thermal Analysis Results

Figure 5 shows the current density distribution of the IGBT chip at 60s. For a more precise description, we encoded each bonded interface in the form of i-j, as shown in Figure 5 (a), where i represents the encoding of the bonding wires from left to right, and j represents the encoding of the bonded interface on the bonding wires from top to bottom. From Figure 5 (b), it can be seen that the current density around the bonded interface is higher. The current density value at the i-2 bonded interface is greater than that at the i-1 bonded interface. The current density around the bonded interface of 2-j, 8-j, and 9-j is significantly higher than others. The current density is highest at 8-2, with a maximum value of 1074A/mm^2. In addition, we found a significant correlation between the magnitude of current density and the distance from the bonded interface to the edge of the chip. The farther the bonded interface is from the edge of the chip, the higher the current density.

Figure 6 shows the temperature curve with the time increase and the temperature distribution of the module at the 60th second. As the diagram shows, the temperature gradually increases during the cycle when the current is activated and then decreases when the current is deactivated. As the loading time increases, the maximum temperature gradually increases and stabilizes in the fifth cycle. The highest temperature at this time is 154°C. The temperature distribution shows a gradually decreasing trend from the center to the edge of the chip.

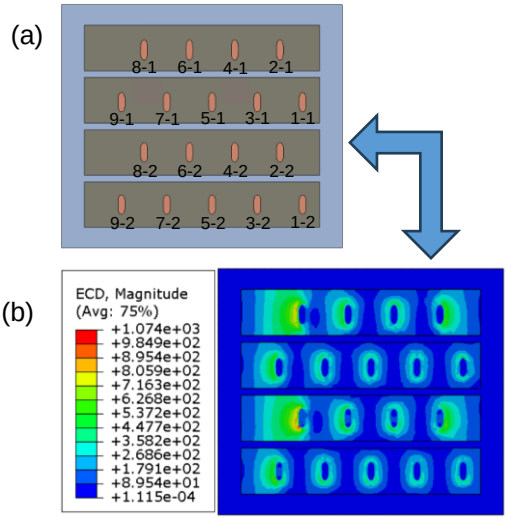

Fig. 5. The results of Current density distribution of the IGBT chip. (a) The schematic of encoded bonding interface; (b)simulation results.

 DOI:10.30420/566414030

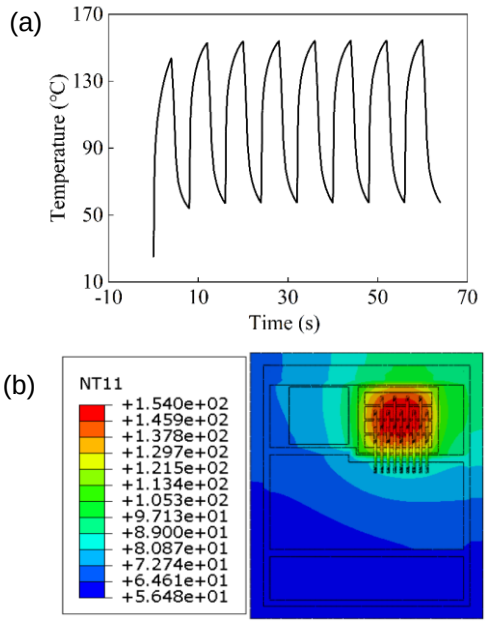

Fig. 6. The temperature results within the IGBT module. (a) Temperature curve of IGBT central node; (b) Temperature distribution at 60s.

3.2 Thermal-mechanical Analysis Results

After applying the temperature results of the electro-thermal analysis to the model, the thermal-mechanical results can be obtained, as shown in Figure 7. It shows the equivalent plastic strain distribution of the bonding wire at the end of the 8th cycle. It can be seen that the equivalent plastic strain of the second bonding point is always greater than that of the first bonding point. Using the encoding method as shown in Figure 5 (a), it can be represented as i-2>i-1. In addition, long bonding wires have a greater equivalent plastic strain than short bonding wires. The maximum equivalent plastic strain occurs at the outermost edge of the second bonding point of the long bonding wire (i.e., encoded 4-2), with a value of approximately 0.1983. From the von Mises stress distribution results shown in Figure 7 (b), it is found that it is consistent with the law of equivalent plastic strain mentioned above. The maximum von Mises stress is located at the outermost edge of the second bonding point of the long bonding wire (i.e., encoded 4-2), with a value of approximately 71.24MPa. This indicates that the 4-2 bonding wire is more likely to fail. Figure 8 shows the cumulative equivalent plastic strain history at the 4-2 bonding interface. As we can see, the accumulated equivalent plastic strain gradually increases.

From the above analysis, it can be seen that the maximum equivalent plastic strain and von Mises stress occur at the edge of the bonded interface between the Al bonding wires and the Si chip, where cracks may start and propagate along the interface until fatigue failure occurs. The reason for this phenomenon is the significant difference in CTE between Al and Si. In addition, based on the temperature distribution results mentioned above, we found that the junction temperature of the 4-2 bonded interface is the highest compared to other bonding interfaces. Therefore, this may be the reason for the maximum von Mises stress and equivalent plastic strain at the 4-2 bonded interface.

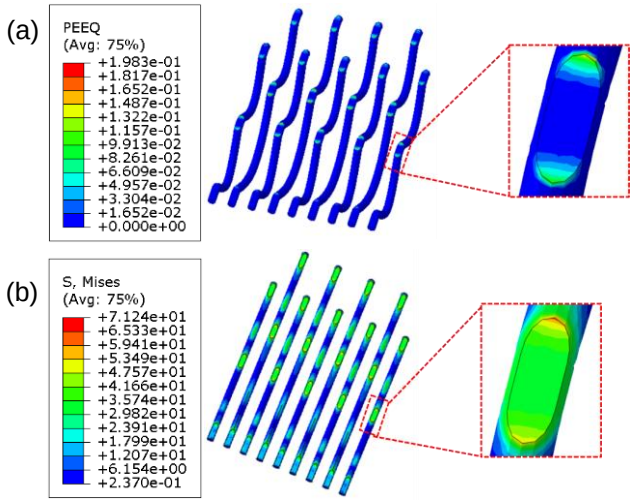

Fig. 7. The results of thermal-mechanical analysis. (a) Equivalent plastic strain distribution of the bonding wires, (b) von Mises stress distribution of the bonding wires.

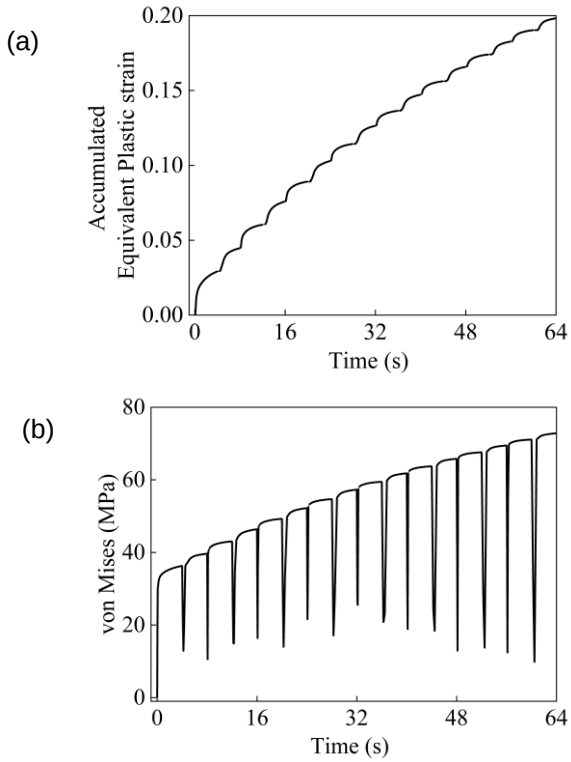

Fig. 8. The results of strain/stress history of the 4-2 bonded interface. (a) Accumulated Equivalent Plastic strain; (b) von Mises stress.

3.3 Effect of bonded interface damage on mechanical and electro-thermal characteristic

The above analysis is the situation where the damage is 0%. In this section, a mechanical analysis was conducted on the finite element models with damage of 10%, 30%, 70%, and 90% to study the effect of bonded interface damage on mechanical and electro-thermal characteristics. The mechanical and electro-thermal parameters analyzed in this paper included temperature, turn-on voltage, current density, and displacement for these IGBT models. Figure 9 shows the change of mechanical and electro-thermal parameters with increased damage. It can be seen from the graph that as the damage increases, all parameters gradually increase. Compared with the results of the 0% damage model, these parameters increased by 0.58%, 0.65%, 128.5%, and 1.89%respectively, with the most significant increase in current density.

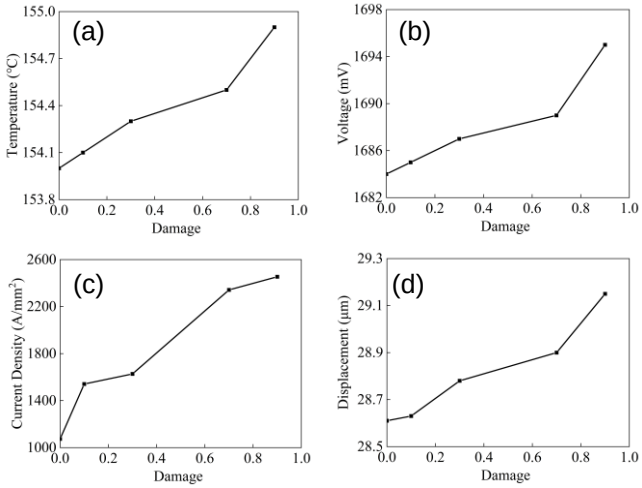

Fig. 9. The effect of the bonded interface damage on mechanical and electrothermal characteristic. (a) Effect on temperature, (b) Effect on turn-on voltage, (c) Effect on current density, (d) Effect on displacement of boding wires.

4 Conclusions

1) The electro-thermal analysis results indicate a significant correlation between current density and the distance from the bonding interface to the edge of the chip. The farther the bonding interface is from the edge of the chip, the higher the current density. The IGBT module's maximum temperature is at the chip's center. The temperature fluctuations within the module become stable after five cycles.
2) The thermal-mechanical results indicate that the maximum equivalent plastic strain occurs at the edge of the bonded interface, where the cracks may initiate and then propagate along the interface.
3) The bonded interface damage simulation results indicate that the maximum temperature and the turn-on voltage do not significantly increase with the increase in the bonded interface damage area. However, the bonding wire's current density and displacement significantly increase.

5 References

[1] N. Iwamuro, T. Laska. IGBT history, state-of-the-art, and future prospects. IEEE Transactions on Electron Devices. 2017, 64(3): 741-752.

[2] H. Oh, B. Han, P. McCluskey, C. Han, et al. Physics-of-Failure, Condition Monitoring, and Prognostics of Insulated Gate Bipolar Transistor Modules: A Review. IEEE Transactions on Power Electronics. 2015, 30(5): 2413-2426.

[3] L. Xie, E. Deng, S. Yang, Y. Zhang, Y. Zhong, Y. Wang, Y. Huang. State-of-the-art of the bond wire failure mechanism and power cycling lifetime in power electronics, Microelectronics Reliability. 2023, 147.

[4] T. Yamaguchi, Y. Suto, N. Araki, M. Eto, et al. Investigation of failure mechanism of aluminum scandium wire bond contact under active power cycle test. Microelectronics Reliability. 2023, 144: 114956.

[5] J. M. Thebaud, E. Woirgard, C. Zardini, S. Azzopardi, et al. Strategy for designing accelerated aging tests to evaluate IGBT power modules lifetime in real operation mode, IEEE Transactions on Components and Packaging Technologies. 2003, 26(2): 429-438.

[6] A. Halouani, Z. Khatir, M. Shqair, A. Ibrahim, P. Pichon. An EBSD Study of Fatigue Crack Propagation in Bonded Aluminium Wires Cycled from 55°C to 85°C. Journal of Electronic Materials. 2022, 51: 7353–7365.

[7] X. Bie, F. Qin, T. An, J. Zhao, and C. Fang. Numerical simulation of the wire bonding reliability of IGBT module under power cycling. 2017 18th International Conference on Electronic Packaging Technology (ICEPT), Harbin, China, 2017, pp. 1396-1401.